Optimized Parameters Initialization of a RMRAC Controller Applied to Grid-Connected Converters

Guilherme V. Hollweg
University of Michigan - Dearborn
hollweg@umich.edu, guilhermehollweg@ieee.org

Paulo J. D. de O. Evald
Federal University of Pelotas

E. Mattos, L. C. Borin, R. V. Tambara and V. F. Montagner
Federal University of Santa Maria

***Abstract*—This work aims to present a proposal for optimized initialization of parameters with the aid of meta-heuristics of a Robust Model Reference Adaptive Controller (RMRAC). Since adaptive controllers need their initialization of gains and constants for proper tuning of the controller, and this choice of gains is related to the designer's experience, the use of optimization algorithms to choose a suitable set of parameters for the controller is viable, because in addition to presenting optimized performance for the application, it becomes independent of the designer's experience in tuning the parameters. For optimal tuning of the RMRAC, a Genetic Algorithm (GA) is used, and the controller is applied to the current regulation of a single-phase power converter connected to the grid with an LCL filter. Simulation results are presented, which shows the effectiveness of the proposal when compared to a RMRAC initialized empirically by an expert designer.**

***Keywords* – Automatic Controllers, RMRAC, Grid-tied Converter, LCL filter.**

I. Introduction

The increasing demand for electrical energy in human activities and the concerns with environmental preservation lead higher integration of renewable energy sources into the grid [1]. The control of subsystems related to grid-connected converters (GCCs) has been developed in the last decades [2]. In this context, the control of the grid-injected currents is an important issue, allowing to regulate the power flow between the primary source and the grid [3].

One of the most common configuration of grid-connected converters is the voltage source inverter with LCL filter, due to its high capacity of reducing pulsed-width (PWM) modulation harmonics due to high attenuation of the filter. However, this topology demands a proper damping of the LCL filter resonance, which can be obtained by means of passive methods or active methods [4]–[6]. Among active damping, the proportional-integral and proportional-resonant controllers are widely used, but have as a common problem the potential reduction of performance when operating under varying parameters, as, for instance, grid impedance variations at the point of common coupling (PCC) [5], [7]

Robust controllers have been developed for GCCs, based on fixed or in adaptive control gains [4], [8], [9]. Although fixed gains lead to simpler control algorithms, they can have lower performance when compared with time-varying control gains from adaptive strategies [10].

A common problem of direct type adaptive controllers is the initial choice of initialization parameters (adaptation gains Γ, κ, λ, etc., as well as adaptive parameters of $\boldsymbol{\theta}$). As discussed in the literature, the random choice of initialization parameters, even if the stability conditions are respected, do not guarantee good regulation performance, and can lead to instability in face of parametric variations, disturbances or severe overshoot [11], [12]. So, this work proposes the optimized initialization of an RMRAC controller through meta-heuristics, with the aid of Genetic Algorithms (GA). The adaptive structure is simulated through a GA until there is a solution set that meets the stability condition, as well as the design constraints added by the designer. In this way, an optimized set of parameters that regulate the plant properly is found. The obtained results are implemtend and compared with that obtained by a well-experienced designer.

II. System Description

This section will present the system description, as well as the plant transfer function and the converter parameters. The electric circuit diagram is presented in Figure 1, where i_{Lc}, i_{cf} and i_{Lg} are the currents flowing through the inverter-side inductor L_c, capacitor and grid-side inductor L_g, respectively. Moreover, r_c and r_g are the parasitic resistances associated to L_c and L_g, respectively. Thereby, L_{g2} is the electrical grid inductance and R_{g2} is its parasitic resistance, which are unknown in practice. In addition, v_g and i_{Lg2} are the corresponding values for grid voltage and grid-injected current, respectively. By means of simplification, i_{Lg2} is considered equal to i_{Lg}. Finally, S_1 to S_4 are the converter switches and v_{link} is the DC bus voltage. Note that the plant is a single-phase grid-tied VSI with an LCL filter. In Figure 1 is presented the whole diagram, simila to what can be implemented in Hardware in the Loop (HIL) or experimentally. However, this work will present simulation results in Matlab, so the dynamics of grid synchronization and PWM are not considered. The VSI was considered as case of study, but other power converter topologies could be implemented, once the controller is designed considering mostly the LCL filter model.

The LCL filter modeling is well known in the literature [8], [9], then it will be omitted in this work. The transfer function that relates the current injected into the grid (i_{Lg}) and the

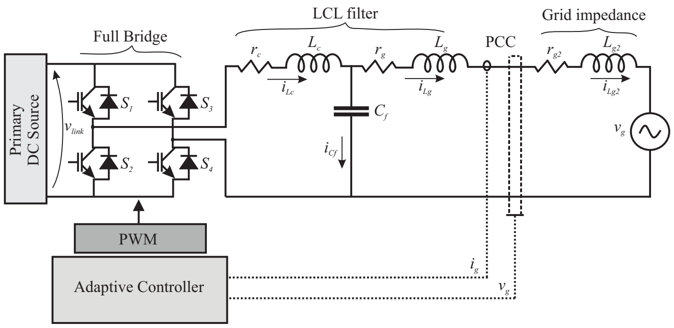

Figure 1. Electrical diagram of single-phase VSI with an LCL filter.

voltage synthesized through modulation ($\bar{v}_{ab}$) is

$$\frac{i_{Lg}(s)}{\bar{v}_{ab}(s)} = \frac{\dfrac{1}{L_g L_c C_f}}{s^3 + \dfrac{(r_g L_c + r_c L_g)}{L_g L_c} s^2 + \dfrac{(L_c + L_g + r_g r_c C_f)}{L_g L_c C_f} s + \dfrac{r_g + r_c}{L_g L_c C_f}}. \quad (1)$$

The design of the output filter elements was made according to [13], following the proposed constraints and the steps for design an adequate LCL filter. The filter parameters, as well as the other relevant parameters, are shown on Table I, where P_{in} is the converter full power and T_s is the sampling frequency.

Table I
PARAMETERS OF THE POWER CONVERTER

Parameter	Value	Parameter	Value
P_{in} (max.)	2.69 kW	f_s	5.04 kHz
L_c	1 mH	r_c	0.05 Ω
L_g	1 mH	r_g	0.05 Ω
L_{g2}	1 mH	r_{g2}	0.05 Ω
C_f	62 μF	V_{link}	400 V
V_g	127 V	I_{Lg}	21.21 A

III. RMRAC CONTROLLER

This section will present the RMRAC controller equations, as well as the simplification model of the plant and the reference model design.

The control law can be described by

$$\boldsymbol{\theta}^T(k)\boldsymbol{\omega}(k) + r(k) = 0, \quad (2)$$

where $r(k)$ is the reference signal, $\boldsymbol{\theta}(k)$ is the adaptive gains vector and $\boldsymbol{\omega}(k)$ is a regressor vector. Also, $\boldsymbol{\omega}(k)$ can be described as $\boldsymbol{\omega}(k) = [\ \boldsymbol{\omega}_1(k)\ \boldsymbol{\omega}_2(k)\ y(k)\ u(k)\ ]^T$, where $\boldsymbol{\omega}_1(k)$ and $\boldsymbol{\omega}_2(k)$ are

$$\begin{aligned} \boldsymbol{\omega}_1(k+1) &= (\boldsymbol{I} + \boldsymbol{F}T_s)\boldsymbol{\omega}_1(k) + \boldsymbol{q}u(k), \\ \boldsymbol{\omega}_2(k+1) &= (\boldsymbol{I} + \boldsymbol{F}T_s)\boldsymbol{\omega}_2(k) + \boldsymbol{q}y(k), \end{aligned} \quad (3)$$

where $\boldsymbol{I}$ is an $n \times n$ identity matrix and $(\boldsymbol{F}, \boldsymbol{q})$ is a controllable pair with an stable matrix $\boldsymbol{F}$ and a controllable parameters vector $\boldsymbol{q}$, with $(n_p - 1) \times (n - 1)$ and $(n - 1)$ dimensions, respectively [14].

Since the nominal part of the plant is considered to be a first-order transfer function, even though the plant is of third order, then there is no $\boldsymbol{\omega_1}$ e $\boldsymbol{\omega_2}$. Then, $\boldsymbol{\omega}(k) = [\ u(k)\ y(k)\ ]^T$. However, to deal with the grid voltages, which were not considered in the plant modeling, one can consider them as an exogenous and periodic disturbance [8], [9]. In this way, $\boldsymbol{\omega}(k) = [\ u(k)\ y(k)\ \ V_s(k)\ V_c(k)\ ]^T$, where $V_s(k)$ and $V_c(k)$ are the grid voltages in phase and quadrature, respectively. Thus, there are two parameters to be adapted from the reference model and two parameters referring to the grid voltages. Then, the gain vector can be rewritten as $\boldsymbol{\theta}(k) = [\ \theta_u(k)\ \ \theta_y(k)\ \theta_s(k)\ \ \theta_c(k)\ ]^T$.

Expanding the terms of (2), considering the first-order reference model, we have the implementable control action, as

$$u(k) = \frac{-\theta_y(k)y(k) - \theta_c(k)V_c(k) - \theta_s(k)V_s(k) - r(k)}{\theta_u(k)}. \quad (4)$$

The parameter adaptation algorithm is of the Gradient type, as

$$\boldsymbol{\theta}(k+1) = \boldsymbol{\theta}(k) - T_s\sigma(k)\boldsymbol{\Gamma}\boldsymbol{\theta}(k) - T_s\ \kappa\frac{\boldsymbol{\Gamma}\boldsymbol{\zeta}(k)\epsilon(k)}{m^2(k)}, \quad (5)$$

where the augmented error $\epsilon(k)$ is

$$\epsilon(k) = e_1(k) + \boldsymbol{\theta}^T(k)\boldsymbol{\zeta}(k) - y_m(k), \quad (6)$$

and the auxiliar gains vector is $\boldsymbol{\zeta}$, according to

$$\boldsymbol{\zeta} = W_m(z)\boldsymbol{\omega}, \quad (7)$$

where $e_1(k)$ is the tracking error, as $e_1 = y(k) - y_m(k)$. A majorant is considered to ensure that the closed loop system signals are bounded, and can be written as

$$\bar{m}^2(k) = m^2(k) + \boldsymbol{\zeta}^T(k)\boldsymbol{\Gamma}\boldsymbol{\zeta}(k), \quad (8)$$

with

$$m(k+1) = (1 - T_s\delta_0)m(k) + T_s\delta_1(1 + |u(k)| + |y(k)|), \quad (9)$$

while $m(0) > \delta_1/\delta_0$ e $\delta_0 + \delta_1 \leq min[p_0, q_0]$. Moreover, $\delta_1 > 0$ and $q_0 > 0$ so that the poles of $W_m(z - q_0)$ and the eigenvalues of $F + q_0\boldsymbol{I}$ are stable, and $0 < p_0 < 1$ is the known lower bound on the stability margin of p, where p are the poles of $\Delta_m(z - p)$, $\Delta_a(z - p)$ are stable [14].

In order to accelerate the convergence of adaptation gains, increasing the dynamics of the system, a positive factor κ is used in (5). In addition, a σ-modification function was incorporated into the parameter adaptation algorithm to increase the robustness of the system and prevent the adaptation gains from drifting during the starting transient [15]. The σ-modification function is

$$\sigma(k) = \begin{cases} 0 & \text{if} \quad \|\boldsymbol{\theta}(k)\| < M_0 \\ \sigma_0\left(\dfrac{\|\boldsymbol{\theta}(k)\|}{M_0} - 1\right) & \text{if} \quad M_0 \leq \|\boldsymbol{\theta}(k)\| < 2M_0, \\ \sigma_0 & \text{if} \quad \|\boldsymbol{\theta}(k)\| \geq 2M_0 \end{cases} \quad (10)$$

while $M_0 > \|\boldsymbol{\theta}^*\|$ is the upper bound of the norm of $\boldsymbol{\theta}(k)$, oversized for lack of knowledge of $\|\boldsymbol{\theta}^*\|$ and σ_0 is the maximum value of the modification function. More information about the controller equations can be found in [14], [16].

A. Plant Model simplification and Reference Model Design

In [16] a plant simplification for LCL filters was presented, which allowed the design of a first order reference model for direct type adaptive controllers. This same technique was implemented sucessfully in [9], [17] and will be also considered in this work.

To perform the discretization of the system, the *ZOH* method is used. In the case analyzed, the frequency of the electrical grid and consequently of the regulated currents is 60 Hz and the switching frequency of the switches is 5.04 kHz. Discretizing (1), considering the implementation delay of 1 cycle and the converter parameters, it is obtained

$$G_{\bar{v}_{ab}}^{i_{Lg}}(z) = \frac{0.0152z^2 + 0.05713z + 0,01507}{z(z^3 - 1.965z^2 + 1.956z - 0.9826)}. \quad (11)$$

Disregarding the LCL filter capacitor and rewriting (1), follows the simplified model of the continuous-time plant, $G_0(s)$, just like

$$G_0(s) = \frac{769.2}{(s + 76.92)}. \quad (12)$$

Considering the simplified plant presented in (12), first order, the reference model, which dictates the desired dynamics of the signal to be controlled, can also be of first order, with great freedom for its choice [16]. The reference model was chosen with a gain of 0 dB in the dynamics of interest, in order not to apply any gain to the signal to be tracked. Also, the reference model adopted has a real pole two decades above the real pole of the plant, so that it presents a fast dynamics in the current regulation. The chosen $W_m(s)$ reference model can be written as

$$W_m(s) = \frac{8300}{(s + 8300)} . \quad (13)$$

For discrete time, considering the ZOH method and sampling period of 5.04 kHz, the simplified discrete-time plant, $G_0(z)$, which only considers the dynamics of the real pole of the complete plant, $G(z)$, is

$$G_0(z) = \frac{0.1515}{(z - 0.9849)}. \quad (14)$$

Discretizing the reference model presented in (13), one can obtain $W_m(z)$, as

$$W_m(z) = \frac{0.8073}{(z - 0.1927)} . \quad (15)$$

Figure 2 presents the Bode Diagram of the simplified model of the complete plant, $G(z)$, the plant simplified model, $G_0(z)$, and the designed reference model.

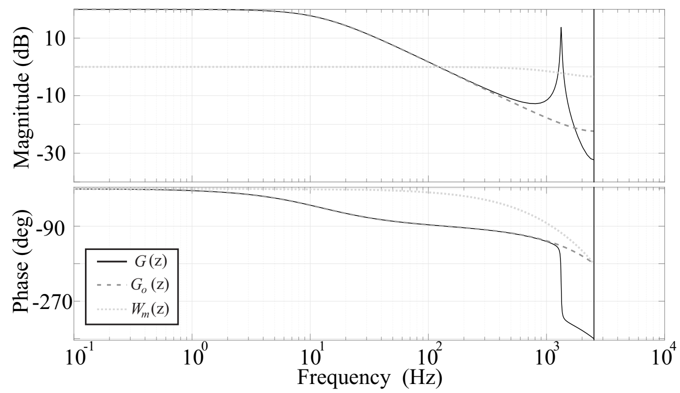

Figure 2. Bode diagram of complete plant, $G(z)$, simplified model of the plant, $G_0(z)$, and reference model, $W_m(z)$.

IV. Optimized initialization of controller parameters with the aid of meta-heuristics

This section will present the optimized initialization procedure using GA, applied for the RMRAC. For the control problem addressed here, the chromosome is given by

$$\mathbf{K}^0 = [\ \Gamma^0 \quad \kappa^0 \quad \theta_u^0 \quad \theta_y^0 \quad \theta_c^0 \quad \theta_s^0\ ] , \quad (16)$$

where the zero superscript in the chromosome and at each gene represents the initial generation. Since the population is generated randomly, the GA can provide simultaneous searches at different points in the space, covering the entire space of solutions [18]. During the execution, the chromosomes that present the best characteristics (lowest fitness) generate new offspring, improving the average fitness of the population using three genetic operators: selection, crossover, and mutation (for more information, please see [19], Subsection III.*A*).

Due to the stochastic nature of the process, GA can converge to different results or even be confined to a local minimum. To mitigate this problem, large populations and different values for mutation and crossover operators can be chosen to ensure population diversity and convergence. Moreover, elitism ensures the reinsertion of the chromosomes with best fitness for the next generation [18], [19]. The GA routine is executed here using the function *ga*, from MATLAB©, in order to find out optimal initial control parameters, shown in (16), for the RMRAC-ASTSM structure.

A. GA Routine for Optimal Parameter Initialization

The Genetic Algorithm optimization routine is employed in the RMRAC controller applied in the grid-side current control of a VSI with LCL filter using MATLAB©. For simplicity, this implementation disregards the dynamics of PWM modulation, as well as the Kalman Filter that will be implemented in the future experimentally. These differences occur from the mathematical model considered to the physical model; but, it is assumed that the adaptive controller is robust enough to ensure performance considering these unmodeled dynamics.

The objective of the proposed design procedure is to obtain a robust adaptive controller with optimized initialization parameters, capable of providing robust stability and adequate

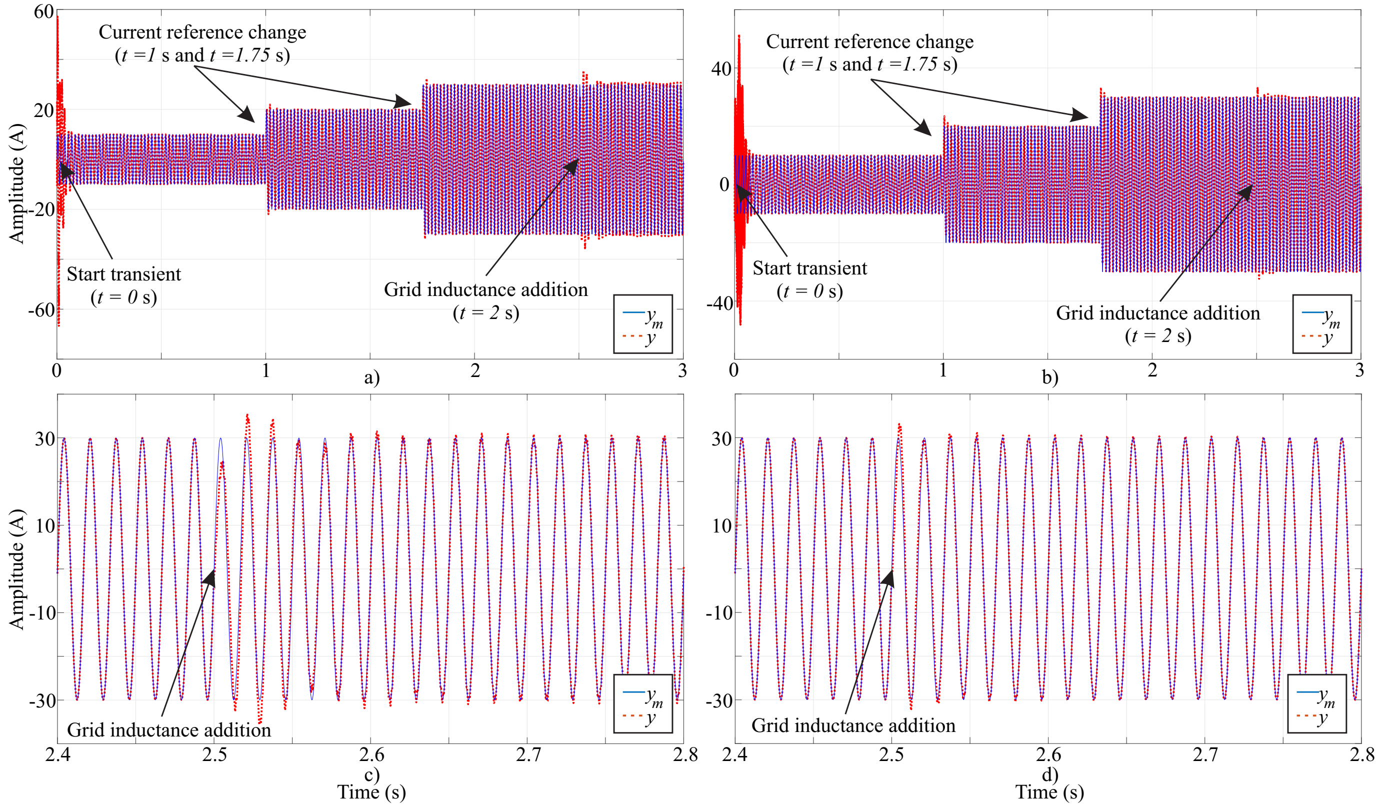

Figure 3. Reference Model output (y_m) and regulated current (y) obtained with both empirically and GA tuned adaptive structures. a) Overall view of the experiment with empirically tuned RMRAC; b) Overall view of the experiment with GA tuned RMRAC; c) Detail of the grid inductance addition instant with empirically tuned RMRAC; d) Detail of the grid inductance addition instant with GA tuned RMRAC.

dynamic performance for GTIs with LCL filter subject to uncertainties in the grid inductance, L_{g2}, making adaptive controller tuning less dependent on designer expertise. The optimization of the adaptive controller can be achieved through the following optimization problem

$$\mathbf{K}^{\star} = \arg \min_{\mathbf{K} \in \mathcal{K}} F(\mathbf{K}), \tag{17}$$

where $\mathcal{K}$ is the search space defined for the parameters and $F(\mathbf{K})$ is the cost function, according to

$$F(\mathbf{K}) = \text{IAE}. \tag{18}$$

The IAE method is the integral of the absolute value of the tracking error, $e_1(k)$, implemented as

$$\text{IAE} = \textstyle\sum_{k=N_1}^{N_2} |e_1(k)| \,, \tag{19}$$

where N_1 and N_2 are the initial and final samples, defined by the designer according to the execution time of the optimization routine.

The GA algorithm was executed using the *ga* function from MATLAB©, considering 100 chromosomes and 600 generations, a mutation rate of 1% and elitism between generations. The lower search limit of the parameter vector to be optimized is $K_{inf} = [1\ 1\ \ -10\ \ -10\ \ -10\ \ -10\ ]$. The upper search limit is $K_{sup} = [\ 5^3\ \ 5^3\ \ 10\ \ 10\ \ 10\ \ 10\ ]$. This process has a duration of 3 s and load steps were performed during the simulation, from 10 A_{pk} to 20 A_{pk}, and later from 20 A_{pk} to 30 A_{pk}. With the system at full load (30 A_{pk}), it was also added a grid inductance of 1 mH, referring to a weaker grid environment. Therefore, the GA algorithm will seek a solution set of parameters that minimizes the tracking error considering these plant dynamics differences.

It is highlighted that if the found out solution set did not meet stability constraints presented in [14], the fitness function is penalized with 1×10^{30}. It is also penalized if the tracking error (e_1) and augmented error (ϵ), in steady state (with currents at 10 A, 20 A and 30 A), exceeds 1 A, because there are considerable persistent errors. In this case, the applied penalty is 1×10^{20}. In addition, if the control action exceeds 1000 V, when the system is in steady state, there will also be a penalty of 1×10^{20}. Note that these steady state penalties do not depend on whether the system has 10 A, 20 A or 30 A. They occur cumulatively, all with a value of 1×10^{20}, aiming to exclude the solution sets that did not meet the imposed conditions in the parametrization. Note also that the penalty applied when the solution set does not meet the stability constraint is greater than the penalties if the system performance is not adequate, associating with the vector gains $\boldsymbol{K}$ with evolve to instability a large value of cost function.

V. Simulation Results

In this section, MATLAB© simulation results of the current control of a single-phase grid-tied VSI with an LCL filter are presented. The results obtained with the RMRAC controller with optimized initialization through the GA are compared with an RMRAC controller empirically designed by an experienced designer. Note that the simulation results do not consider the PWM or the grid-synchronization dynamics.

The simulation routine is the same as presented in the previous section. The GA obtained optimized parameters were: $\mathbf{\Gamma} = 1$, $\kappa = 4998.002305$, $\theta_u(0) = -2.125155$, $\theta_y(0) = -1.88623$, $\theta_c(0) = 0.25942$ and $\theta_s(0) = 2.31557$. The empirically tuned RMRAC have the following parameters: $\mathbf{\Gamma} = 1$, $\kappa = 1000$, $\theta_u(0) = -3$, $\theta_y(0) = -0.01$, $\theta_c(0) = 1$ and $\theta_s(0) = 3$. Also, for both adaptive structures were considered $M_0 = 5$ and $\sigma_0 = 0.1$, according to [9].

Figure 3 shows the Reference Model output (y_m) and regulated current (y) obtained with both empirically and GA tuned adaptive structures. Note that both controllers designed regulate the plant, as shown in Figures 3a) and b). However, it is observed that the structure with parameters initialized by the GA presented better regulation gain after the grid inductance parametric variation, according to Figures 3c) and d). It is noted that the regulated current overshoot observed with the tuned structure with the aid of meta-heuristics is reduced, as well as a better steady-state regulation performance with the system at full load in a weaker grid environment, where the plant output most closely follows the reference model.

Figure 4 presents the tracking error (e_1) obtained with both empirically and GA tuned adaptive structures. It can be observed that the empirically regulated adaptive structure presents greater overshoots during the load steps and mainly during the addition of inductance in the grid, at $t = 2.5$ s. Furthermore, a residual error is noticeable in the empirically regulated structure that is not noticed in the RMRAC with parameters tuned with the aid of the GA. This occurs since a set of gains that regulates the plant in situations where there is no unmodeled dynamics does not guarantee stability in situations with unmodeled dynamics, as discussed in [11]. Therefore, it is interesting to test an adaptive controller in different situations, including the presence of unmodeled dynamics and disturbances in the plant.

Figure 5 shows the adaptive gains vector $\boldsymbol{\theta}$ obtained with both empirically and GA tuned RMRAC structures. Note that the gains of both controllers converge in steady state. Furthermore, it can be seen that some gains of the regulated structure with meta-heuristics present high transients at the start, but quickly converge to limited values. This shows that there is still room for performance improvement in the results obtained with the aid of meta-heuristics, varying the upper and lower limits of the $\boldsymbol{K}$ chromosome or adding new restrictions and penalties in the optimized initialization routine.

VI. Conclusion

This work presented a proposal for a design procedure for optimized initialization of parameters of adaptive controllers

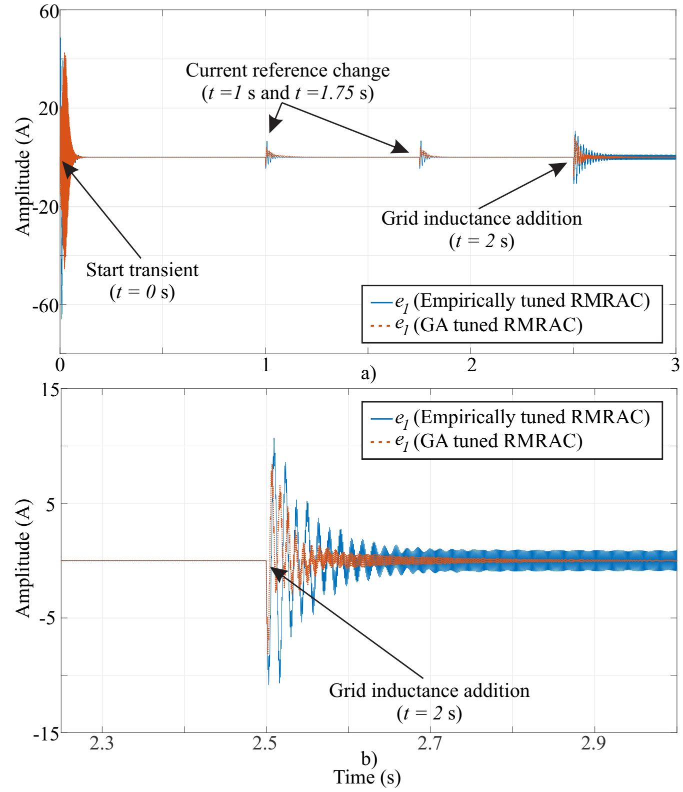

Figure 4. Tracking error (e_1) obtained with both empirically and GA tuned adaptive structures. a) Overall view of the experiment; b) Detail of the grid inductance addition instant at t=2.5 s.

with the aid of metaheuristics. As a case study, the procedure was implemented in a RMRAC controller for tuning 6 parameters. The controller was applied to the current regulation of a single-phase VSI converter grid-connected with an LCL filter. Simulation results were presented comparing the RMRAC structure GA tuned with a RMRAC empirically tuned by an experienced designer. Based on the presented results, a significant improvement can be observed in the current regulation performance in a weaker grid environment, when an inductance of 1 mH is added to the grid, reducing the overshoot, as well as the steady-state current error. In addition, it is observed that there is room for improvement in the results, where other optimization algorithms can be tested, as well as other cost functions. Also, it is possible to test other lower and upper limits of the parameters to be optimized and modify the restrictions and penalties in the GA routine. Finally, this technique is not restricted to RMRAC controllers and single-phase VSI converters, it could also be applied in the regulation of other adaptive structures and other types of plants.

References

[1] R. Teodorescu, M. Liserre, and P. Rodríguez, *Grid Converters for Photovoltaic and Wind Power Systems*, ser. Wiley - IEEE. John Wiley & Sons, 2011.

[2] F. Blaabjerg, R. Teodorescu, M. Liserre, and A. Timbus, "Overview of control and grid synchronization for distributed power generation systems," *IEEE Transactions on Industrial Electronics*, vol. 53, no. 5, pp. 1398–1409, oct. 2006.

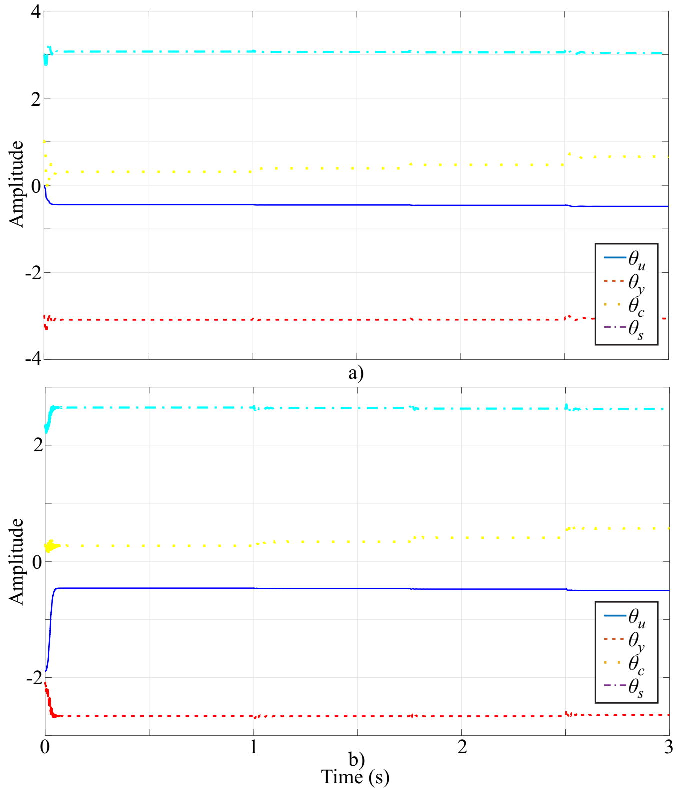

Figure 5. Adaptive gains vector $\boldsymbol{\theta}$ obtained with both adaptive control structures. a) Empirically tuned RMRAC; b) GA tuned RMRAC.

[3] A. Timbus, M. Liserre, R. Teodorescu, P. Rodriguez, and F. Blaabjerg, "Evaluation of current controllers for distributed power generation systems," *IEEE Transactions on Power Electronics*, vol. 24, no. 3, pp. 654–664, Mar. 2009.

[4] M. Liserre, F. Blaabjerg, and S. Hansen, "Design and control of an LCL-filter-based three-phase active rectifier," *IEEE Transactions on Industry Applications*, vol. 41, no. 5, pp. 1281–1291, 2005.

[5] M. Liserre, A. Dell'Aquila, and F. Blaabjerg, "Genetic algorithm-based design of the active damping for an LCL-filter three-phase active rectifier," *IEEE Transactions on Power Electronics*, vol. 19, DOI 10.1109/TPEL.2003.820540, no. 1, pp. 76 – 86, jan. 2004.

[6] J. Dannehl, M. Liserre, and F. Fuchs, "Filter-based active damping of voltage source converters with LCL filter," *IEEE Transactions on Industrial Electronics*, vol. 58, no. 8, pp. 3623–3633, Aug. 2011.

[7] J. Dannehl, F. Fuchs, and P. Thøgersen, "PI state space current control of grid-connected PWM converters with LCL filters," *IEEE Transactions on Power Electronics*, vol. 25, no. 9, pp. 2320–2330, sept. 2010.

[8] J. R. Massing, M. Stefanello, H. A. Gründling, and H. Pinheiro, "Adaptive current control for grid-connected converters with LCL filter," *IEEE Transactions on Industrial Electronics*, vol. 59, no. 12, pp. 4681–4693, 2012.

[9] G. V. Hollweg, P. J. D. de Oliveira Evald, R. V. Tambara, and H. A. Gründling, "A robust adaptive super-twisting sliding mode controller applied on grid-tied power converter with an LCL filter," *Control Engineering Practice*, vol. 122, p. 105104, 2022.

[10] K. J. Astrom and B. Witternmark, *Adaptive Control*. New York: Dover Publications, 1995.

[11] P. Ioannou and P. Kokotovic, "Robust redesign of adaptive control," *IEEE Transactions on Automatic Control*, vol. 29, no. 3, pp. 202–211, 1984.

[12] P. Ioannou and J. Sun, *Robust Adaptive Control*. New York: Dover Publications, 2012.

[13] A. Reznik, M. G. Simões, A. Al-Durra, and S. Muyeen, "Lcl filter design and performance analysis for grid-interconnected systems," *IEEE Transactions on Industry Applications*, vol. 50, no. 2, pp. 1225–1232, 2013.

[14] P. Ioannou and K. Tsakalis, "A robust discrete-time adaptive controller," in *25th IEEE Conference on Decision and Control*, pp. 838–843, 1986.

[15] R. Lozano-Leal, J. Collado, and S. Mondle, "Model reference robust adaptive control without a priori knowledge of the high frequency gain," in *1988 American Control Conference*, pp. 754–759. IEEE, 1988.

[16] P. J. D. O. Evald, R. V. Tambara, and H. A. Gründling, "A direct discrete-time reduced order robust model reference adaptive control for grid-tied power converters with LCL filter," *Brazilian Journal of Power Electronics*, vol. 25, no. 3, pp. 361–372, 2020.

[17] D. M. C. Milbradt, G. V. Hollweg, P. J. D. O. Evald, and H. A. Gründling, "A robust adaptive one sample ahead preview controller for grid-injected currents of a grid-tied power converter with an LCL filter," *International Journal of Electrical Power & Energy Systems*, vol. 142, p. 108286, 2022.

[18] F. H. Dupont, V. F. Montagner, J. R. Pinheiro, H. Pinheiro, S. V. G. Oliveira, and A. Péres, "Comparison of linear quadratic controllers with stability analysis for DC-DC boost converters under large load range," *Asian Journal of Control*, vol. 15, no. 3, pp. 861–871, 2013.

[19] S. E. De León-Aldaco, H. Calleja, and J. A. Alquicira, "Metaheuristic optimization methods applied to power converters: A review," *IEEE Transactions on Power Electronics*, vol. 30, no. 12, pp. 6791–6803, 2015.